ZIBELINE INTERNATIONAL™ PUBLISHING

ISSN: 2716-5655 (Online)
CODEN: BDWRAP

Big Data in Water Resources Engineering (BDWRE)

DOI: http://doi.org/10.26480/bdwre.01.2025.07.18

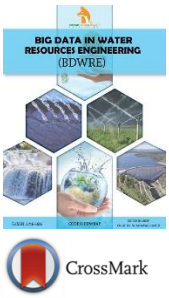

CrossMark

REVIEW ARTICLE

SPATIOTEMPORAL ASSESSMENT OF DROUGHT USING STANDARDIZED PRECIPITATION INDEX (SPI) AND STANDARDIZED PRECIPITATION EVAPOTRANSPIRATION INDEX (SPEI) IN PAKISTAN

Hassnain Haider[a,b], Muhammad Asad Hussain[c], Ali Hasan Jaffry[d], Fakher Abbas[e], Muhammad Burhan Khalid[f], Anas Farooq[g], Iqra Zainab[g], Muhammad Bilal Zahid[h]

[a] School of Ecology and Applied Meteorology, Nanjing University of Information Science and Technology, 210044 Nanjing, Jiangsu, China.
[b] College of Agriculture, University of Sargodha, Sargodha, Punjab, Pakistan.
[c] State Key Laboratory of Climate System Prediction and Risk Management, Nanjing University of Information Science and Technology, Nanjing, 210044, China.
[d] School of Remote Sensing and Geomatics Engineering, Nanjing University of Information Science and Technology, 210044 Nanjing, Jiangsu, China.
[e] Xinjiang Institute of Ecology and Geography, Chinese Academy of Sciences, Urumqi 830011, China.
[f] School of Atmospheric Physics, Nanjing University of Information Science and Technology, 210044 Nanjing, Jiangsu, China.
[g] School of Atmospheric Sciences, Nanjing University of Information Science and Technology, 210044 Nanjing, Jiangsu, China.
[h] School of Environmental Science and Engineering, Nanjing University of Information Science and Technology, 210044 Nanjing, Jiangsu, China.
[*]Corresponding Author Email: asadhussain417@gmail.com

ARTICLE DETAILS

Article History:

Received 04 May 2025
Revised 10 June 2025
Accepted 25 July 2025
Available online 03 August 2025

ABSTRACT

Climate change has been intensifying droughts throughout Pakistan's essential water source region, the Upper Indus River Basin (UIRB). This study evaluates spatiotemporal drought patterns (1982–2014) using SPI and SPEI at 1- to 12-month scales across 11 stations. SPEI demonstrates superior performance over SPI when detecting droughts produced by temperature variations, since it shows better accuracy of 20 to 30%. Results indicate that northern high-altitude regions, including Astore and Dir, experience worsening drought conditions because we use rainfall as precipitation so the regions which have low rainfall are demonstrate drought areas in this study. The Modified Mann-Kendall test shows central and northern parts of UIRB are drying out, as demonstrated by Astore's SPEI-12 dropping at a rate of −0.35 decade^{-1}. The Modified Mann-Kendall test shows significant drying patterns throughout central/northern UIRB, where Astore experienced SPEI-12 declines equal to -0.35 decade^{-1}. Precipitation prediction achieves better accuracy when using Multivariable Linear Regression instead of Partial Least Squares Regression (PLSR) because its RMSE value is slightly lower, and it reveals that temperature and longitude are vital predictors. The number of drought occurrences from 2001 to 2014 at Mangla Reservoir reached 54 events, while it remained at 9 events from 1982 to 1990. The UIRB remains susceptible to drought conditions caused by rising temperatures, thus requiring SPEI-based monitoring systems to implement adaptive water resource management practices. The framework applies to mountainous basins worldwide when fighting droughts that result from climate change.

KEYWORDS

Drought, Upper Indus Basin (UIB), Partial Least Squares Regression (PLSR), Multivariable Linear Regression (MLR)

1. INTRODUCTION

Long periods of reduced rainfall define droughts as natural events that disrupt water systems and create a range of socio-ecological impacts (Portela, et al., 2015). Worldwide droughts have increased in frequency as well as intensity and geographical coverage since global warming quickened, while the California 2012–2015 drought and the East African 2010–2011 famine are among the most disastrous events recorded (Waheed, et al., 2024; Hao, et al., 2018). The pressing need for a better understanding of drought patterns becomes evident because these natural crises often occur where agriculture intersects with vulnerable environmental systems (Iqbal, 2022). The drying conditions faced by South Asia continue to intensify because this region depends on the monsoon for its rains, and glacier loss continues at an accelerated rate (Lutz, et al., 2016). Pakistan stands as one of the five most vulnerable countries to climate change within this specific region (Climate and Development Knowledge Network and Germanwatch, 2020). The author examines Pakistan's Upper Indus River Basin because it provides water to more than 200 million people while investigating drought systems and climate influences to establish adaptation practices.

The global temperature rise, together with unsteady precipitation and elevated evapotranspiration, causes fundamental changes to hydrological systems, which increases drought risks (Iqbal, 2023; Ficklin, et al., 2022). South Asian renewable water resources will decrease by 20–30 %, according to the predictions of the Intergovernmental Panel on Climate

Quick Response Code	Access this article online	
	Website: www.bdwre.com.my	**DOI:** 10.26480/bdwre.01.2025.07.18

Cite The Article: Hassnain Haider, Muhammad Asad Hussain, Ali Hasan Jaffry, Fakher Abbas, Muhammad Burhan Khalid, Anas Farooq, Iqra Zainab, Muhammad Bilal Zahid (2025). Spatiotemporal Assessment of Drought Using Standardized Precipitation Index (Spi) and Standardized Precipitation Evapotranspiration Index (Spei) in Pakistan. *Big Data in Water Resources Engineering, 6(1): 07-18.*

Change (IPCC) for the year 2050, thus escalating water stress across the Indus Basin region (IPCC, 2019). Regions experiencing drought now face years-long emergencies that generate interconnected disasters, which include agricultural meltdowns, diminishing groundwater supplies, and extensive population shifts (Mahla, et al., 2019; Hussain, 2020). A drought in Balochistan, Pakistan, from 1997 to 2003 led to the displacement of 1.2 million people as well as a 40% reduction in wheat yields through 2003; both effects demonstrated severe problems with water governance (Adnan, and Khan, 2009). The impacts become more severe in transboundary basins such as UIRB because glacial meltwater, which supports dry-season flows, continues to decrease rapidly (Azam, and Khan, 2016; Ahmad, 2024).

The Upper Indus River Basin (UIRB), situated between the Himalayas and Karakoram, provides 80% of Pakistan's irrigation via the Indus River System, underpinning national food and water security (Ansari, et al., 2024; Zafar, 2024). This hydrologically critical region exhibits exceptional climate sensitivity, with temperatures rising 1.1°C since 1960, twice the global average, exacerbating water stress (Ashraf, et al., 2023). Approximately 34% of Pakistan's agriculture relies solely on rainfall, heightening vulnerability to drought-induced crop failures (Iqbal, 2022). Despite its ecological and economic importance, UIRB remains understudied compared to downstream plains. Conventional drought monitoring in Pakistan predominantly uses the Standardized Precipitation Index (SPI), which ignores temperature impacts on evapotranspiration (Ahmadzadeh, et al., 2022). This is particularly problematic in mountainous zones like UIRB where warming accelerates moisture loss beyond global averages, leading to systematic underestimation of drought severity (Sebbar, 2024). While the Standardized Precipitation Evapotranspiration Index (SPEI) resolves this by integrating temperature-driven evapotranspiration (Vicente-Serrano, et al., 2010), its application in topographically complex UIRB is limited. Sparse meteorological stations, localized microclimates, and delayed streamflow responses to high-altitude precipitation deficits further challenge accurate drought detection (Rafiq, et al., 2023). Though MLR and PLSR models show promise for isolating drought drivers (elevation, longitude, temperature) based on RMSE/R^2 metrics (Hussain, et al., 2024), they remain underutilized in UIRB studies. Comprehensive drought assessment thus requires integrating SPEI with distributed hydrological modeling and expanded monitoring networks to address UIRB's unique climatological complexities.

This study addresses three critical gaps in drought research: (1) the lack of integrated SPI/SPEI analysis in the topographically complex region of UIRB, (2) an insufficient spatially explicit drought zoning framework for policy, and (3) a limited mechanistic understanding of precipitation drivers in the mountainous basin. To fill these gaps, we computed SPI and SPEI of UIRB at four timescales (1-,3-,6, and 12-month) and from 1982-2014 (Objective 1), applied the MM-K test to resolve contradictory trends from 1982-2014 (Objective 2), mapped hotspots for localized interventions (Objective 3), and used MLR and PLSR to untangle topographic drivers (Objective 4). The combined research approaches establish actionable information to develop multiple drought prevention methods in UIRB.

2. Materials and Methods

2.1 Study area

The Indus River Basin crosses several national borders as it extends throughout four regions, with Pakistan taking up 47% and India covering 39%, while China controls 8% of the territory and Afghanistan maintains 6% (Shamim, et al., 2024) . The UIRB comprises mountainous terrains of the Karakorum, Himalayan, and Hindu Kush Mountain ranges. The UIRB is a hydrological area located in northern Pakistan that encompasses the headwaters of the Indus River. UIRB has an area of around 192,861 km^2, and the mountainous region has an elevation of approximately 6,800m (Baig, et al., 2022). The region serves as a critical water source for downstream agriculture, hydropower, and domestic use. In this study, we use 11 Meteorological stations around UIRB. It includes Astore, Balakot, Bunji, Chitral, Chilas, Dir, Gilgit, Kakul, Mangla, Murree, and Skardu. The selected stations range from the lowest station at 282 m (Mangla) to the highest station at 2317 m (Skardu), as shown in Table 1.

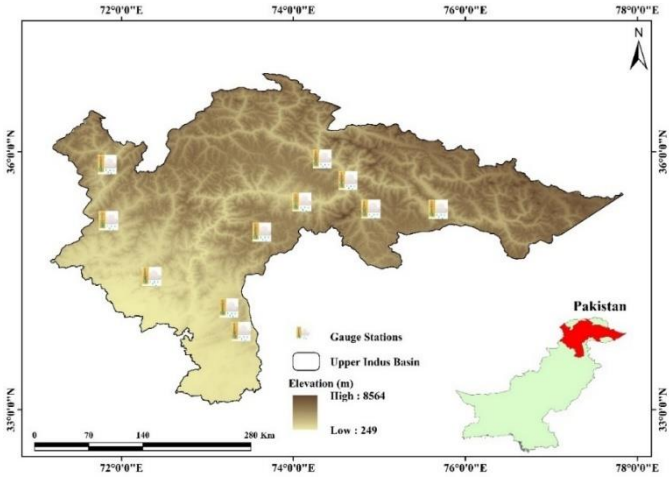

Figure 1: Elevation Map of Upper Indus basin River (UIRB).

2.2 Data collection

Monthly temperature and precipitation data (1982-2014) from 11 PMD stations across UIRB were preprocessed, with anomalies removed and missing values filled using spline interpolation to ensure data continuity.

Table 1: Geographical Stations of Upper Indus River Basin.

Sr. no	Station	Lat (dd)	Lon (dd)	Elevation (m)
1	Astore	35.33	74.90	2168
2	Balakot	34.55	72.35	995.5
3	Bunji	35.66	74.63	1372
4	Chitral	35.85	71.83	1497.8
5	Chilas	35.41	74.10	1250
6	Dir	35.20	71.85	1375
7	Gilgit	35.91	74.33	1460
8	Kakul	34.18	73.25	1308
9	Mangla	35.06	73.63	282
10	Murree	33.90	73.39	2206
11	Skardu	35.33	75.68	2317

2.3 Calculation of Evapotranspiration

We calculate PET using the Thornthwaite method. The Thornthwaite method uses mean temperature (C) to estimate PET, as shown in Equation (1) (Thornthwaite, 1948).

$$i = \left(\frac{t}{5}\right)^{1.514} \quad (1)$$

Where t is the mean monthly temperature. The Annual Heat Index (I) is calculated as the sum of the Monthly Heat Index (i):

$$I = \sum_{i=1}^{12} i \quad (2)$$

A Potential Evapotranspiration (PET) estimation is obtained for each month, considering a month is 30 days long and there are 12 theoretical sunshine hours per day, applying the following equation:

$$PET_{non\ corrected} = 16\left(\frac{10 \cdot t}{I}\right)^{\alpha} \quad (3)$$

Where α is

$$\alpha = 675 \cdot 10^{-9} \cdot I^3 - 771 \cdot 10^{-7} \cdot I^2 + 1792 \cdot 10^{-5} \cdot I + 0.49239$$

Obtained values are later corrected according to the actual length of the month and the theoretical sunshine hours for the latitude of interest, with the formula:

$$PET = PET_{non\ corrected} \cdot \frac{N}{12} \cdot \frac{d}{30} \quad (4)$$

N: are the theoretical sunshine hours for each month and d is the number of days for each month.

2.4 Calculation of the Standardized Precipitation Index (SPI)

The drought condition of an area can be estimated using the Standardized Precipitation Index (SPI) (Kamruzzaman, 2022). The SPI is very easy to use, and it requires a particular dataset (Mckee, et al., 1993). SPI uses precipitation data to calculate drought. McKee and his team developed the Standardized Precipitation Index (SPI) in 1993 (Mckee, et al., 1993). This is based on the chance of precipitation for a few consecutive months, and its main aim is to represent the deficiency of rainfall in an area on various time scales compared with its climatology. Although the SPI approach was not developed as a drought forecasting tool, the SPI method has been used to identify dry or wet conditions (Table 2) and assess their effects on water resources management. The detailed SPI calculating methodology can be found in (Mckee, et al., 1993; Guttman, 1999; Hayes et al., 1999). The SPI has been used in several studies to analyze droughts[31]. The precipitation frequency data from meteorological stations undergoes fitting through a two-parameter gamma distribution function, which analyses values on a single-month basis. This paper demonstrates the application of the gamma distribution function. We use DrinC software to obtain SPI values.

2.5 Calculation of the Standardized Precipitation Evapotranspiration index (SPEI)

This paper introduced a basic concept of a multiple-scale drought index called the SPEI that integrates precipitation and temperature. The SPEI is simple to compute and derived from the original SPI calculation process. The values that are used to calculate the SPI include monthly precipitation data. The SPEI employs the difference between precipitation and PET at a monthly time scale. This climatic water balance is computed on different time scales to arrive at the SPEI, as pointed out by (Thornthwaite, 1948).

The SPEI intensity scale produces positive and negative values to determine dry and wet conditions. Its measurement allows users to select time intervals from one month to more than 12 months for calculation purposes. The system enables operational use through monthly updates, while the increased length of time series data produces more reliable outcomes.

The SPEI value relies on normalizing the water balance difference through a log-logistic probability distribution. The following equation represents the expression of the probability density function.

$$f(x) = \frac{\beta}{\alpha}\left(\frac{x-\gamma}{\alpha}\right)\left[1 + \left(\frac{x-\gamma}{\alpha}\right)\right]^{-2} \quad (5)$$

The parameters α, β, and γ represent scale, shape, and origin, respectively. Thus, the probability distribution function can be described as a probability density function.

$$F(x) = \left[1 + \frac{\alpha}{x-\gamma}\right]^{-1} \quad (6)$$

Defined the SPEI as follows:

$$SPEI = W - \frac{C_0 + C_1 W + C_2 W^2}{1 + d_1 W + d_2 W^2 + d_3 W^3} \quad (7)$$

When $P > 0.5, W = \sqrt{-2\ln(1-P)}$ and when $P \le 0.5, W = \sqrt{-2\ln(P)}$, $C_0 = 2.5155, C_1 = 0.8028$, $C_2 = 0.0203$, $d_1 = 1.4327$, $d_2 = 0.1892$, $d_3 = 0.0013$ (Vicente-Serrano et al., 2010).

Python libraries were used to identify the SPEI at different timescales. The drought severity was assessed by analyzing SPI/SPEI values presented in Table 2. When observed through SPI/SPEI values, rainfall reduction aligns with drought conditions, while SPEI values indicate typical wet conditions upon rainfall increases.

Table 2: Drought Classification based on SPI and SPEI values.

SPEI and SPI values	Drought category
– 1.0 to –1.49	Moderate drought
– 1.5 to –1.99	Severe drought
≤ – 2	Extreme drought

2.6 Runs Theory

The dry period's' length, the water deficit's strength, and the recurrence frequency define drought characteristics. The drought assessment depends heavily on SPI/SPEI under normal conditions (SPI/SPEI ≥ – 1), evaluated using a standard methodology during absolute SPI/SPEI computation. The absolute value of SPI/SPEI is calculated, which substantially impacts drought assessment. We used Y's run theory to establish a method for measuring drought frequency and intensity levels (Yevjevich, 1967). The run theory creates a segmented section of the drought time series, identifying values below or above predefined thresholds. A positive or negative run comprises a segment of the time series data (Mishra and Singh, 2010). The formula for calculating drought intensity is:

$$S = \frac{\sum_{n=1}^{T}\left|S_{\frac{SPI}{SPEI}} - K\right|}{T} \quad (8)$$

Where S denotes the intensity of drought, $S_{\frac{SPI}{SPEI}}$ Denotes an SPEI or SPI value less than or equal to the drought threshold, K denotes drought threshold, which in this study is set to be less than or equal to – 1, indicating that the severity of the drought is greater than that of moderate drought, and T is the duration of the drought. Drought frequency is a metric for understanding how often drought occurs in this area. Its formula is as follows.

$$DF = \frac{n}{N} \times 100 \quad (9)$$

N represents time detection periods, and n counts drought occurrences in the area.

2.7 Conditional Probability

Event probabilities are measured through conditional probability methods, which determine the likelihood of event outcomes based on facts of previously occurring events. The particular method uses Event A to establish a connection with Event B (Van Fraassen, 1976). However, this study's CP(SPI) refers to the possibility of SPEI occurring during an SPI and vice versa for Cp (SPEI). The formula is as follows.

$$Cp(SPI) = \frac{T_{\frac{SPI}{SPEI}}}{T_{SPEI}} or\ Cp(SPEI) = \frac{T_{\frac{SPEI}{SPI}}}{T_{SPI}} \quad (10)$$

Here T_{SPI} and T_{SPEI} tells the drought period in the study area over time, depending on the SPI/SPEI value, but $T_{SPI/SPEI}$ and $T_{SPEI/SPI}$ show when drought occurred within a region after SPEI/SPI confirms drought events, and SPI/SPEI recalculates drought conditions. The research employed a conditional probability distribution built with copulas for meteorological drought evaluation.

2.8 Trend Test

Hamed Rao introduced the Modified Mann-Kendall test (MMK) and used to estimate the correlation (Hamed, and Rao, 1998). This study used the MMK test to identify the spatiotemporal drought trends around UIRB. This analysis was performed using Python at % significance level of 95% ($p<0.05$).

2.9 Sen's Slope Estimator

The nonparametric Sen's slope (SS) technique (Sen, 1968; Thiel, 2025). This study used this method to estimate the rate of trend magnitude in the datasets and assess the magnitude of the trend. Recent research has proven that this method is less sensitive to outlier effects than other

methods for determining trend outcomes.(Novotny and Stefan, 2007). The Sen's slope (SS) can be calculated using the equation.

$$\beta = Median\left[\frac{x_j - x_i}{j-i}\right] \; all \; j > i \qquad (11)$$

Here, xj denotes the jth value, and xi is the ith value in the observational data. The β value indicates the rate of change; if the value is positive, then the rate increases, and a value negative means a decrease in the rate of change.

2.10 Multivariable Linear Regression Method

Linear multivariable regression involves multiple explanatory variables in the analysis, between the linear and nonlinear regression types (Gupta and Agarwal, 2021). Multivariable linear regression (MLR) is the basis for establishing a multiple regression model that connects meteorological variables with their geographical interpolation aspects. The dependent variable is precipitation (Y), while the independent variables consist of altitude (H), maximum temperature (T_{max}), and minimum temperature (T_{min}), alongside longitude (Lo) and latitude (La) (Ramgopal, et al., 2019; Zhou, et al., 2014). MLR calculated using XLSTAT.

2.11 Partial Least Squares Regression (PLSR)

PLSR was applied by using XLSTAT to overcome multicollinearity issues in MLR. It reduces dimensionality by constructing latent variables from independent predictors before regression. The performance of MLR and PLSR was compared using R^2 and RMSE values.

3. Spatiotemporal Patterns of Drought on Multi-Scale

Figures 2–5 display the spatial distribution of 1-, 3-, 6-, and 12-month SPI and SPEI across the UIRB for 1984, 1994, 2004, and 2014. Negative values (red) indicate drought severity, while positive values (green) reflect wetter conditions. Most of the humid study region experienced wet to mild drought conditions, with slightly drier trends in lower areas post-2000. Both short- and long-term scales (SPI/SPEI) showed consistent mild drought risk, with no severe drought observed during the study period.

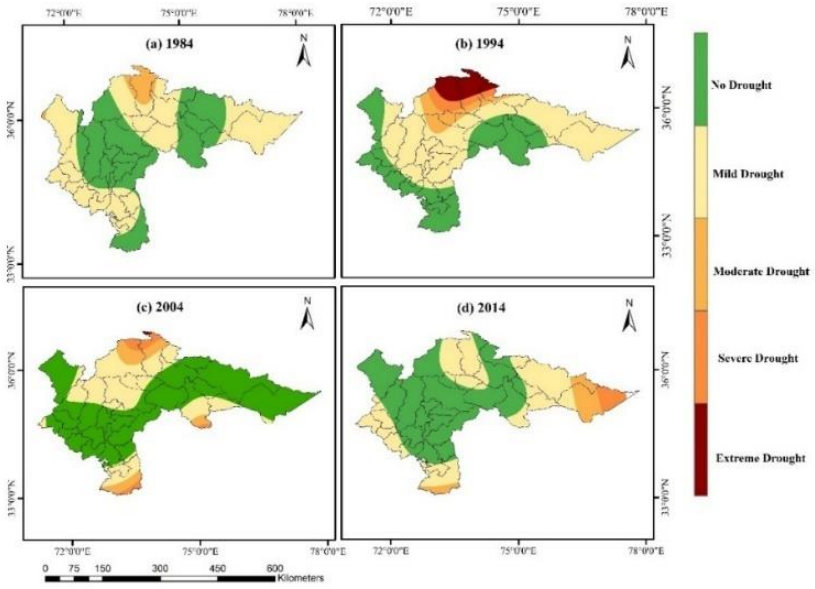

Figure 2: Spatial Distribution of 1-Month SPI Across the Upper Indus River Basin for (a) 1984, (b) 1994, (c) 2004, and (d) 2014. Negative Values (Red Hues) Denote Drought Severity, While Positive Values (Green) Indicate Wetter Conditions.

SPI and SPEI were calculated monthly (1982–2014) at 1-, 3-, 6-, and 12-month scales. The MMK test revealed temporal trends, showing spatial and temporal drought variations across the UIRB. Most catchments exhibited moderate drought in SPEI-1 and SPEI-6, while SPEI-12 indicated severe drought in some areas. The MMK test revealed varying drought trends across stations and timescales (Table 3). Astore showed significant drying trends in SPI and SPEI, especially at the 12-month scale (−0.35 decade^{-1}, $p < 0.05$), highlighting long-term drought intensification in high-altitude areas. Balakot, Dir, and Murree also exhibited negative trends, indicating worsening drought conditions. In contrast, Skardu displayed improved drought conditions, with a significant positive SPEI-12 trend (0.10 decade^{-1}, $p = 0.03$). Mangla experienced severe drying, particularly at the 12-month scale (−0.46 decade^{-1}, $p < 0.05$), suggesting rising temperature-driven drought stress in central regions

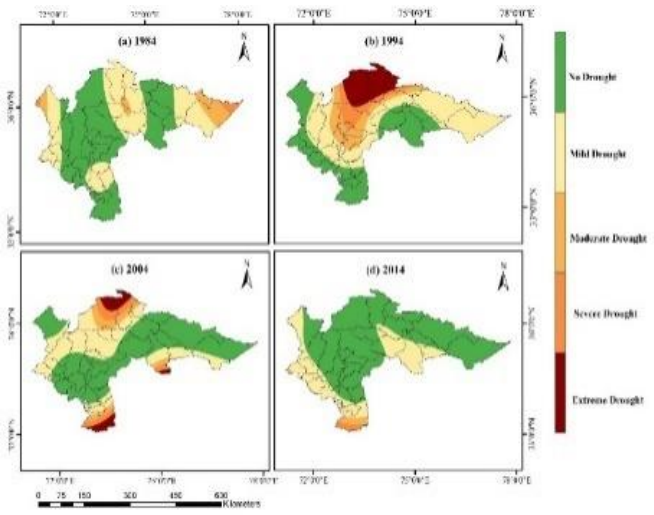

Figure 2: Spatial Distribution of 3-Month SPI Across the Upper Indus River Basin for (a) 1984, (b) 1994, (c) 2004, and (d) 2014. Negative Values (Red Hues) Denote Drought Severity, While Positive Values (Green) Indicate Wetter Conditions.

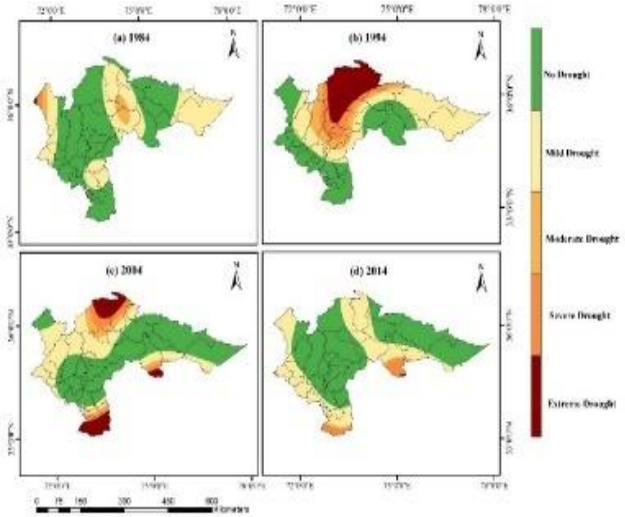

Figure 3: Spatial Distribution of 6-Month SPI Across the Upper Indus River Basin for (a) 1984, (b) 1994, (c) 2004, and (d) 2014. Negative Values (Red Hues) Denote Drought Severity, While Positive Values (Green) Indicate Wetter Conditions.

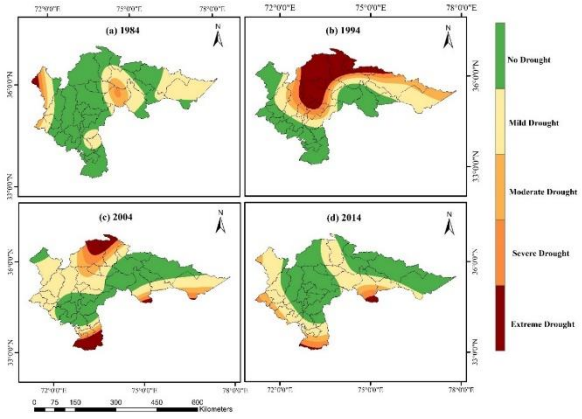

Figure 4: Spatial Distribution Of 12-Month SPI Across the Upper Indus River Basin For (A) 1984, (B) 1994, (C) 2004, And (D) 2014. Negative Values (Red Hues) Denote Drought Severity, While Positive Values (Green) Indicate Wetter Conditions.

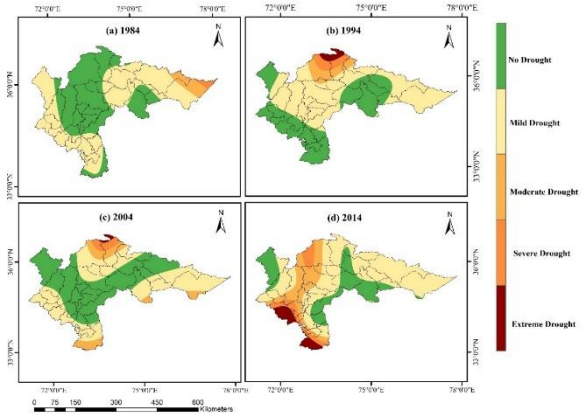

Figure 5: Spatial Distribution Of 1-Month SPEI Across the Upper Indus River Basin For (A) 1984, (B) 1994, (C) 2004, And (D) 2014. Negative Values (Red Hues) Denote Drought Severity, While Positive Values (Green) Indicate Wetter Conditions.

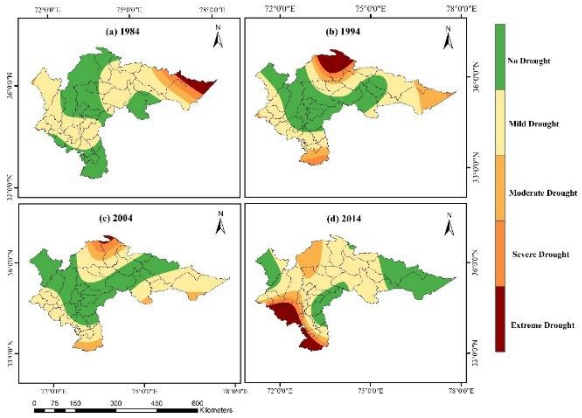

Figure 6: Spatial Distribution Of 3-Month SPEI Across the Upper Indus River Basin For (A) 1984, (B) 1994, (C) 2004, And (D) 2014. Negative Values (Red Hues) Denote Drought Severity, While Positive Values (Green) Indicate Wetter Conditions

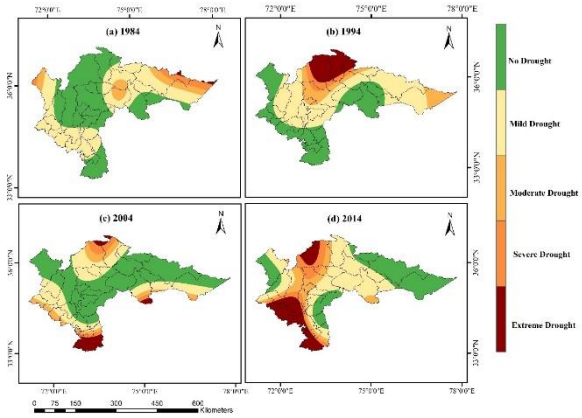

Figure 7: Spatial Distribution of 6-Month SPEI Across the Upper Indus River Basin for (a) 1984, (b) 1994, (c) 2004, and (d) 2014. Negative Values (Red Hues) Denote Drought Severity, While Positive Values (Green) Indicate Wetter Conditions.

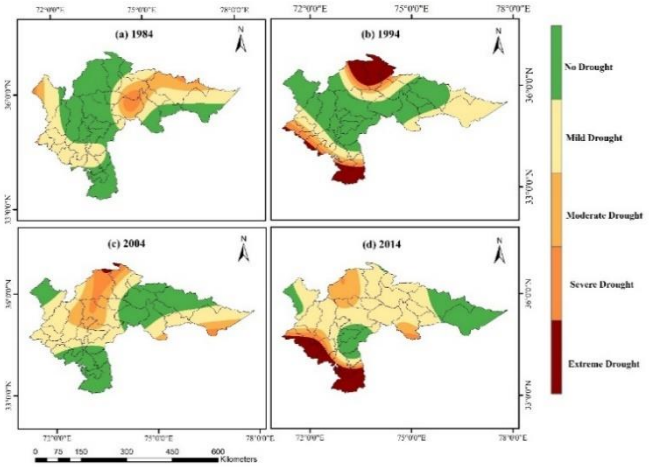

Figure 8: Spatial Distribution of 12-Month SPEI Across the Upper Indus River Basin for (a) 1984, (b) 1994, (c) 2004, and (d) 2014. Negative Values (Red Hues) Denote Drought Severity, While Positive Values (Green) Indicate Wetter Conditions.

Table 3: MMK Trend test coefficient and significant coefficient (P) of SPI and SPEI on various time scales in different regions of UIRB.

Station	SPI scale	Trend (decade-1)	Z value	p-value	SPEI scale	Trend (decade-1)	Z value	p-value
Astore	SPI1	-0.06	-1.15	0.24	SPEI1	-0.08	-1.37	0.16
	SPI3	-0.14	-2.55	0.01	SPEI3	-0.17	-3.02	0.00
	SPI6	-0.19	-3.43	0.00	SPEI6	-0.26	-4.57	0.00
	SPI12	-0.22	-3.67	0.00	SPEI12	-0.35	-6.19	0.00

Table 3 (cont): MMK Trend test coefficient and significant coefficient (P) of SPI and SPEI on various time scales in different regions of UIRB.

Balakot	SPI1	-0.06	-1.19	0.23	SPEI1	-0.13	-2.41	0.00
	SPI3	-0.17	-2.93	0.00	SPEI3	-0.22	-3.79	0.00
	SPI6	-0.21	-3.92	0.00	SPEI6	-0.18	-4.06	0.00
	SPI12	-0.27	-5.19	0.00	SPEI12	-0.33	-6.10	0.00
Bunji	SPI1	0.09	2.14	0.03	SPEI1	0.00	0.04	0.96
	SPI3	0.16	2.76	0.01	SPEI3	0.00	0.08	0.93
	SPI6	0.18	3.18	0.00	SPEI6	0.00	-0.01	0.99
	SPI12	0.16	2.99	0.00	SPEI12	-0.09	-1.50	0.11
Chilas	SPI1	0.14	3.42	0.00	SPEI1	0.12	2.17	0.03
	SPI3	0.19	3.45	0.00	SPEI3	0.14	2.48	0.01
	SPI6	0.16	3.15	0.00	SPEI6	0.15	2.62	0.01
	SPI12	0.28	4.73	0.00	SPEI12	0.18	2.83	0.00
Chitral	SPI1	-0.01	-0.16	0.86	SPEI1	-0.05	-0.97	0.32
	SPI3	-0.01	-0.32	0.77	SPEI3	-0.08	-1.47	0.13
	SPI6	0.01	0.17	0.85	SPEI6	-0.10	-1.81	0.07
	SPI12	0.01	0.08	0.92	SPEI12	-0.13	-2.76	0.00
Dir	SPI1	-0.09	-1.72	0.08	SPEI1	-0.11	-2.19	0.02
	SPI3	-0.22	-4.01	0.00	SPEI3	-0.25	-4.39	0.00
	SPI6	-0.27	-5.38	0.00	SPEI6	-0.23	-5.00	0.00
	SPI12	-0.38	-6.94	0.00	SPEI12	-0.39	-7.02	0.00
Gilgit	SPI1	0.12	2.36	0.07	SPEI1	0.00	-0.03	0.96
	SPI3	0.15	2.83	0.00	SPEI3	0.02	0.38	0.70
	SPI6	0.19	3.46	0.00	SPEI6	0.04	0.88	0.37
	SPI12	0.28	5.09	0.00	SPEI12	0.06	1.01	0.30
Kakul	SPI1	-0.07	-1.36	0.17	SPEI1	0.10	-1.77	0.07
	SPI3	-0.14	-2.60	0.01	SPEI3	-0.12	-2.73	0.01
	SPI6	-0.17	-3.79	0.00	SPEI6	-0.15	-3.60	0.00
	SPI12	-0.26	-5.58	0.00	SPEI12	-0.17	-5.19	0.00
Murree	SPI1	-0.11	-1.96	0.04	SPEI1	-0.11	-2.08	0.03
	SPI3	-0.21	-3.73	0.00	SPEI3	-0.20	-3.55	0.00
	SPI6	-0.31	-5.35	0.00	SPEI6	-0.28	-4.88	0.00
	SPI12	-0.43	-7.29	0.00	SPEI12	-0.40	-6.96	0.00
Skardu	SPI1	0.09	1.75	0.07	SPEI1	0.08	1.44	0.13
	SPI3	0.05	1.14	0.25	SPEI3	0.10	1.75	0.07
	SPI6	0.01	0.26	0.78	SPEI6	0.08	1.47	0.14
	SPI12	0.06	1.60	0.10	SPEI12	0.10	2.07	0.03
Mangla	SPI1	-0.02	-0.61	53.00	SPEI1	-0.14	-2.49	0.01
	SPI3	-0.07	-1.31	0.18	SPEI3	-0.24	-4.18	0.00
	SPI6	-0.09	-1.61	0.10	SPEI6	-0.30	-5.41	0.00
	SPI12	-0.18	-3.26	0.00	SPEI12	-0.46	-8.13	0.00

Table 4: Partial Least Squares Regression results for the whole time period.

Station	**Period**	**Cp (SPI)**				**Cp (SPEI)**			
		1	**3**	**6**	**12**	**1**	**3**	**6**	**12**
Astore	**1982-1990**	0.5	0.75	0.9	0.7	0.8	0.81	0.9	0.87
	1991-2000	0.68	0.78	0.92	0.77	0.68	0.84	0.85	1
	2001-2014	0.74	0.75	0.78	0.87	0.89	0.96	0.87	1
Balakot	**1982-1990**	0.07	0.06	0	0	0.06	0.07	0	0
	1991-2000	0.14	0.06	0	0.16	0.13	0.05	0	0.15
	2001-2014	0.08	0.23	0.17	0	0.1	0.25	0.16	0
Bunji	**1982-1990**	0.14	0.55	0.52	0.5	0.18	0.48	0.58	0.91
	1991-2000	0.07	0.36	0.43	1	0.09	0.25	0.21	0.32
	2001-2014	0.07	0.35	0.39	0.4	0.29	0.55	0.67	0.73

Table 4 (cont): Partial Least Squares Regression results for the whole time period.									
Chilas	**1982-1990**	0.27	0.67	0.67	0.84	0.5	0.61	0.71	0.72
	1991-2000	0.08	0.15	0.27	0.17	0.13	0.18	0.5	0.17
	2001-2014	0	0.19	0.28	0.29	0	0.36	0.63	0.42
Chitral	**1982-1990**	0.64	0.76	1	1	0.58	0.93	0.7	0.75
	1991-2000	0.47	0.75	0.8	/	0.7	0.82	0.36	0
	2001-2014	0.61	0.59	0.81	0.67	0.79	0.65	0.73	0.69
Dir	**1982-1990**	0.89	0.92	1	1	0.8	1	1	0.82
	1991-2000	0.8	1	0.67	/	0.8	1	0.67	/
	2001-2014	0.89	0.83	0.71	0.87	0.97	0.97	0.81	0.92
Gilgit	**1982-1990**	0.15	0.57	0.62	0.57	0.13	0.42	0.53	0.76
	1991-2000	0.47	0.6	0.71	0.75	0.44	0.44	0.68	0.41
	2001-2014	0.31	0.26	0.27	0.3	0.47	0.53	0.82	0.63
Kakul	**1982-1990**	0.84	1	0.75	/	0.89	0.79	0.67	/
	1991-2000	0.69	0.88	0.8	0.75	0.69	0.78	0.67	0.6
	2001-2014	0.75	0.83	0.84	0.87	0.84	0.68	0.9	0.74
Murree	**1982-1990**	0.94	0.86	1	0.91	1	0.86	0.73	0.91
	1991-2000	0.93	0.86	1	/	0.87	1	0.8	/
	2001-2014	0.86	0.9	0.95	0.92	0.88	0.9	0.93	0.92
Skardu	**1982-1990**	0.45	0.5	0.62	0.4	0.53	0.65	0.68	0.9
	1991-2000	0.43	0.5	0.55	0	0.5	0.64	1	/
	2001-2014	0.41	0.63	0.4	0.5	0.7	0.81	0.86	0.9
Mangla	**1982-1990**	0.56	0.79	0.83	/	0.56	0.69	0.45	0
	1991-2000	0.4	0.85	1	1	0.46	0.69	0.26	0.58
	2001-2014	0.43	0.48	0.4	0.37	0.75	0.71	0.62	0.49

Using Conditional Probability (Cp), SPEI demonstrated higher accuracy than SPI in detecting drought across all timescales (1-, 3-, 6-, 12-month). For example, at 1-month scales, SPEI's Cp was notably higher (Astore: 0.68–0.89 vs. SPI's 0.50–0.74; Skardu: 0.53–0.70 vs. SPI's 0.41–0.45), proving its superior sensitivity to temperature-driven droughts. This trend persisted across longer scales, confirming SPEI's robustness in integrating temperature and evapotranspiration effects.

Using the MMK test, we analyzed precipitation trends (1982–2014) across 11 UIRB stations. From 1982–1990, 60% of stations (mainly southern/central low-elevation areas) showed significant declines ($P < 0.05$). During 1991–2000, northern regions like Skardu saw non-significant increases ($P > 0.5$), while 2001–2014 exhibited mixed trends, with 65% of stations recording higher rainfall—particularly in eastern areas (e.g., Skardu).

4. Precipitation Trends over Upper Indus River Basin

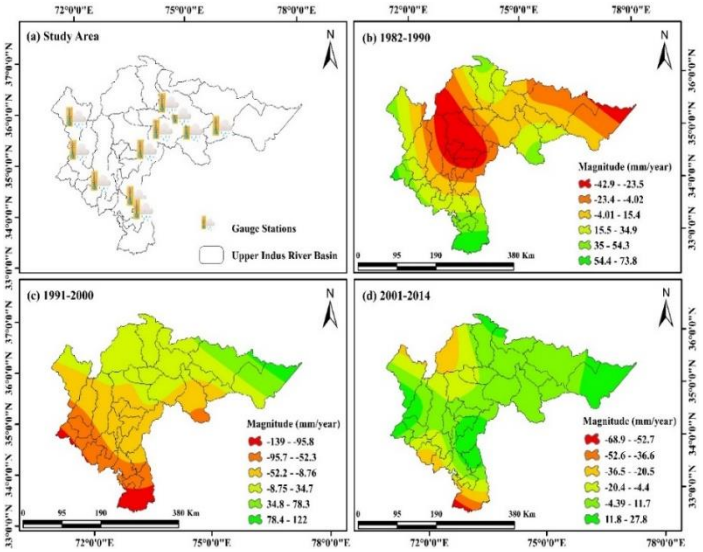

Figure 10: The MMk Trend Test Coefficient for UIRB's Precipitation from a Range of Time Periods (1982-1990, 1991-2000, and 2001-2014).

Over 32 years, the Upper Indus River Basin exhibited distinct precipitation patterns: northern highlands (e.g., Skardu) and eastern areas received higher rainfall, while central/southern regions (e.g., Mangla) showed declining trends. These inconsistent spatial variations suggest influences beyond rainfall alone, potentially linked to land-use changes or atmospheric circulation patterns.

5. Drought Frequency and Intensity Using SPEIs in Different Zones

Using run theory on SPEI data (1982–2014), we analyzed drought characteristics across UIRB. Results showed increasing drought frequency at most stations, except Chilas (southwest), where events decreased from 32 (1982–1990) to 17 (2001–2014) on 12-month scales. The 3-month droughts were most frequent. Intensity peaked (>1.5) in 1982–1990, weakened in 1990–2000, then rose again post-2000, reflecting heightened drought severity in recent years.

Table 5: Drought Intensity and Frequency of UIRB at different Time scales.

Stations	Period	Drought Frequency				Drought Intensity			
		1	3	6	12	1	3	6	12
Astore	1982-1990	16	12	10	10	-1.28	-1.49	-1.53	-1.23
	1991-2000	16	14	13	9	-1.74	-1.54	-1.54	-1.43
	2001-2014	35	40	37	47	-1.6	-1.52	-1.6	-1.64
Balakot	1982-1990	14	15	6	9	-1.42	-1.38	-1.39	-1.97
	1991-2000	21	16	15	12	-1.48	-1.45	-1.51	-1.44
	2001-2014	25	34	34	30	-1.64	-1.58	-1.86	-1.56
Bunji	1982-1990	14	20	21	21	-1.66	-1.47	-1.5	-1.67
	1991-2000	13	14	14	10	-1.55	-1.33	-1.36	-1.15
	2001-2014	26	31	41	40	-1.67	-1.6	-1.45	-1.47
Chilas	1982-1990	26	30	30	32	-1.58	-1.62	-1.67	-1.54
	1991-2000	13	13	15	12	-1.57	-1.51	-1.42	-1.83
	2001-2014	24	21	18	17	-1.46	-1.38	-1.42	-1.28
Chitral	1982-1990	11	17	14	16	-1.6	-1.26	-1.36	-1.26
	1991-2000	15	12	5		-1.44	-1.31	-1.27	
	2001-2014	31	37	36	36	-1.76	-1.62	-1.66	-1.97
Dir	1982-1990	18	13	10	11	-1.44	-1.48	-1.59	-1.15
	1991-2000	15	9	3	0	-1.46	-1.4	-1.19	
	2001-2014	35	42	41	54	-1.57	-1.54	-1.95	-1.49
Gilgit	1982-1990	13	14	13	23	-1.72	-1.56	-1.75	-1.43
	1991-2000	17	20	21	12	-1.46	-1.4	-1.37	-1.44
	2001-2014	26	34	33	33	-1.69	-1.52	-1.52	-1.58
Kakul	1982-1990	19	12	11	3	-1.52	-1.36	-1.35	-2.28
	1991-2000	13	8	5	4	-1.49	-1.5	-1.63	-1.39
	2001-2014	28	30	32	23	-1.53	-1.86	-2.19	-3.04
Murree	1982-1990	17	16	14	15	-1.57	-1.48	-1.66	-1.63
	1991-2000	14	7	4	0	-1.64	-1.5	-1.19	
	2001-2014	35	41	43	53	-1.43	-1.52	-1.44	-1.4
Skardu	1982-1990	20	22	21	25	-1.81	-1.55	-1.66	-1.42
	1991-2000	14	14	11	2	-1.43	-1.39	-1.38	-1.07
	2001-2014	34	27	30	40	-1.58	-1.6	-1.6	-1.67
Mangla	1982-1990	9	15	9	3	-1.77	-1.38	-1.29	-1.82
	1991-2000	15	13	5	7	-1.46	-1.36	-1.43	-1.23
	2001-2014	35	46	45	54	-1.64	-1.58	-1.85	-1.72

6. Spatial Distribution of Drought Intensity and Frequency

SPEI outperformed SPI in detecting drought variability, especially at 1-month scales. Drought frequency rose moderately during 1991–2000 (peak: 21 events in Balakot) before surging sharply in 2001–2014 (35 events at multiple stations). Spatial analysis revealed expanding drought coverage, culminating in widespread dry conditions across UIRB, reflecting intensified severity and geographical spread over time.

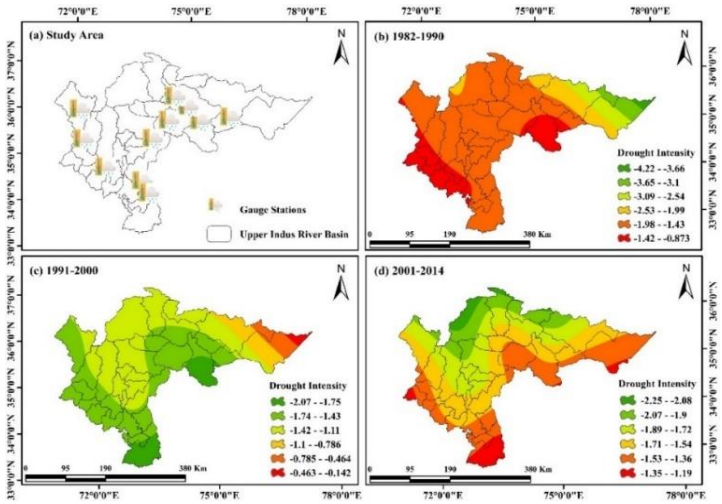

Figure 9: Based on 1-month SPEI, drought intensity during individual decades (1982-1990s, 1991-2000s, and 2001-2014s) in UIRB.

The drought intensity (Figure 3) across 1982–1990 peaked at -1.81 in Skardu and remained at -1.72 in Gilgit and -1.66 in Bunji. The drought intensities in Astore and Chilas proved to be less severe than the other areas, at -1.28 and -1.58, respectively. The intense dryness during this period predominantly affected northern parts of the UIRB and northeastern areas, but left the

southern districts with milder dry conditions. Drought conditions intensified overall during 1991–2000, as the northern and central parts of the UIRB region witnessed increased drought severity. The areas of Murree (-1.64), Bunji (-1.55), and Chilas (-1.57) recorded the most severe droughts, which showed worsening dryness than during the earlier decade. Data shows droughts intensified, yet they did not reach extreme levels across the studied period (-1.43 to -1.74). Rising rainfall but reduced snowfall (suggesting warmer temperatures) coincided with intensifying UIRB droughts from 2001-2014. Drought severity peaked at Chitral (-1.76), followed by Bunji (-1.67) and Gilgit (-1.69), indicating significant moisture decline. Murree (-1.43) and Chilas (-1.46) also showed increasing dryness. Overall, drought conditions worsened substantially basin-wide between 1982-2014, becoming most severe in later years.

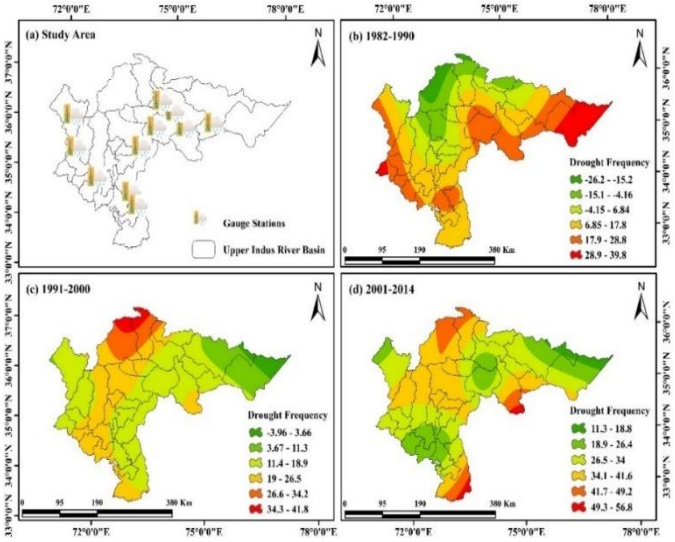

Figure 10: Based on 1-month SPEI, Drought Frequency during individual decades (1982-1990s, 1991-2000s, and 2001-2014s) in UIRB.

7. Multivariable Linear Regression Method

The Multiple Linear Regression (MLR) model was used to assess the influence of geographical and meteorological factors on precipitation across 11 stations in the UIRB. The independent variables included latitude, longitude, minimum temperature (T_{min}), maximum temperature (T_{max}), and elevation, with precipitation as the dependent variable. Table 6 presents the analyzed periods' estimated regression coefficients, standard errors, p-values, and statistical significance. The coefficient of determination (R^2) values ranged from 0.265 to 0.316, indicating that the selected predictors explained 26.5% to 31.6% of the variation in precipitation. For every period, the Root Mean Square Error (RMSE), a critical model performance indicator, was also calculated:

- 1982-1990: RMSE = 85.181
- 1991-2000: RMSE = 78.611
- 2001-2014: RMSE = 67.893

An improvement in model accuracy is indicated by a decreasing RMSE with time, especially in the most recent time frame (2001–2014). Stable model performance was demonstrated by the adjusted R2 values, which did not change over time.

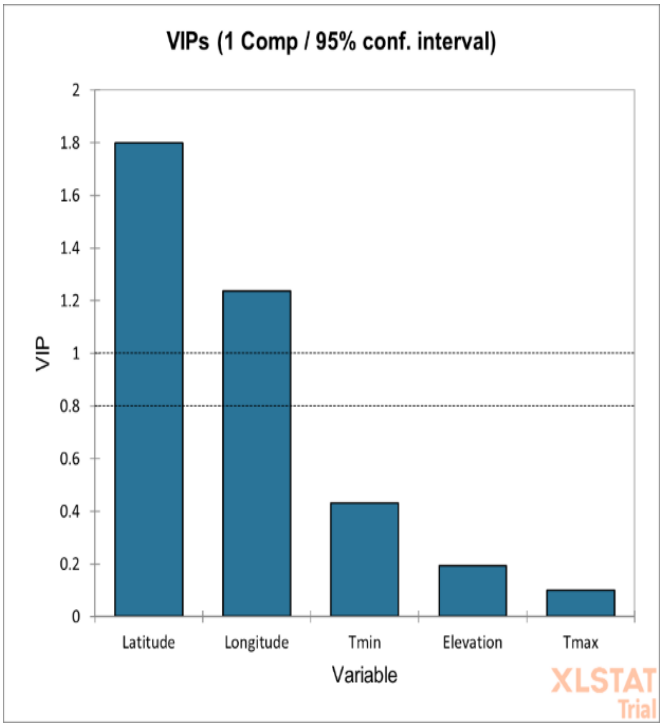

Figure 11: VIP score of all parameters from 1982-1990. longitude latitude have higher values showing have high impacts on the precipitation.

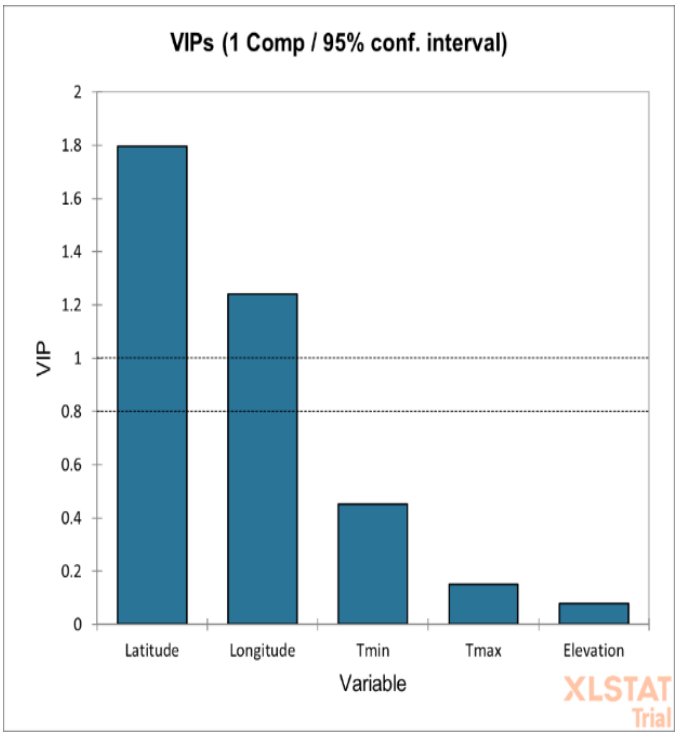

Figure 12: VIP score of all parameters from 1991-2000. longitude, latitude, and Temperature have higher values showing have high impacts on the precipitation.

Table 6: Multivariable Linear Regression results for the whole period.							
Period	**R2**	**RMSE**	**Latitude**	**Longitude**	**T_{min}**	**T_{max}**	**Elevation**
1982-1990	0.26	85.1	-56.4	-19.0	3.0	-2.3	0
1991-2000	0.31	78.6	-56.1	-19.4	4.3	-3.4	0
2001-2014	0.27	67.8	-42.9	-16.3	3.7	-2.9	-0.0

8. Partial Least Squares Regression (PLSR) Results

Partial Least Squares Regression (PLSR) enhanced predictive performance using the same independent variables. Figures 5, 6, and 7 show the variable importance in Projection (VIP) ratings, which show the relative significance of each predictor. Across all periods, latitude and longitude had the highest VIP values, indicating their dominance in precipitation variability. Furthermore, Tmin had a more significant VIP score than Tmax, indicating that the minimum temperature has a more significant influence on the distribution of precipitation in our study area.

- 1982-1990: RMSE = 86.07
- 1991-2000: RMSE = 80.28
- 2001-2014: RMSE = 69.66

MLR showed slightly lower RMSE values than PLSR, indicating better predictive accuracy for precipitation. Both models identified latitude and longitude as dominant influences, with T_{min} contributing moderately. Elevation and T_{max} had minimal impacts, though MLR consistently outperformed PLSR despite small RMSE differences.

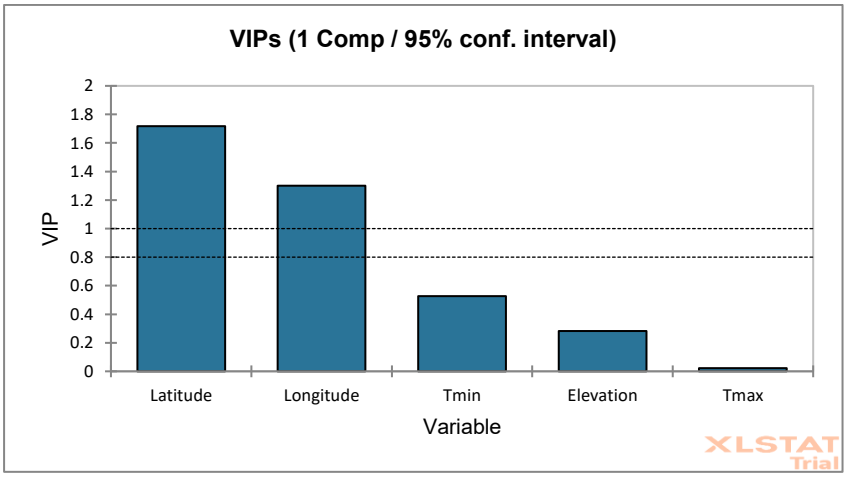

Figure 13: VIP score of PLSR for all parameters from 2001-2014. Longitude, Latitude, and Temperature have higher values showing have an impact on the precipitation.

Table 7: Partial Least Squares Regression results for the whole time period.							
Period	**R2**	**RMSE**	**Latitude**	**Longitude**	**T_{min}**	**T_{max}**	**Elevation**
1982-1990	0.24	86.07	-55.6	-20.0	1.0	-0.1	-0.0
1991-2000	0.28	80.28	-58.1	-21.0	1.1	-0.3	-0.0
2001-2014	0.23	69.66	-41.1	-16.2	0.9	0.0	-0.0

9. Discussion

The research results show how climatic conditions and terrain features determine hydrological risks through time and space in the Upper Indus River Basin. Studies show that the Standardized Precipitation Evapotranspiration Index (SPEI) proves more effective than the Standardized Precipitation Index (SPI) because it assesses drought by incorporating temperature-related characteristics in a warming climate. The incorporation of potential evapotranspiration (PET) in SPEI integrates rising temperature effects with moisture shortages in ways that match global drought observations about how single-precipitation indices fail in areas with substantial warming (Vicente-Serrano, et al., 2010; Ougahi, et al., 2022). Since 1960, the UIRB region has experienced temperature increases that exceed twice the global rate, which thus increases evapotranspiration rates while intensifying drought conditions across areas like Astore and Dir (Ashraf, et al., 2023; Rafiq, 2024; Dubey, et al., 2023; Hussain, et al., 2024).

The drought patterns across UIRB show contrasting effects between the northern and central dry zone and the southern wet zone because of the basin's physical landscape and climatic patterns. The higher elevation positions of northern stations reveal erosion between temperature rise in the area and precipitation gains from vertical weather patterns, which scientists call the "elevation paradox." (Gao, 2021). The close location of Mangla to monsoon moisture sources reduces the impact of temperature changes on its drought occurrences, although drought frequency is increasing. The monsoon precipitation in Pakistan depends on geographic orientation, where eastern Himalayan valleys (including Skardu and Gilgit) attract more rainfall because they align with moisture-bearing winds from eastern India, yet western Himalayan valleys (like Chitral) remain dry due to their obstructing terrain (Adnan et al., 2022).

Linear predictability among climatic triggers (such as temperature and longitude) and hydrological outcomes in the UIRB demonstrates why MLR succeeds as a predictor over PLSR. The simpler linear model of MLR displayed better predictive performance with 67.9 RMSE compared to PLSR's 69.7 RMSE during 2001–2014, because distinct topographical boundaries and climate zones in the region display minimal predictor interaction according to [39]. Analysis results show that maximum temperature negatively influences adequate water availability across all timescales (−2.326 to −3.49) regardless of rainfall stability.

Drought events at Mangla surged from 9 to 54 post-2000, reflecting escalating water scarcity across South Asia. Ground-based meteorological data, while robust, lacks spatial precision in complex terrains. Future research must integrate satellite datasets (e.g., GRACE, MODIS) to resolve local climate dynamics beyond rainfall metrics and support adaptive water management.

10. Conclusion

This study examines drought patterns in the UIRB (1982–2014), showing how rising temperatures and geographic longitude drive precipitation shifts and worsening droughts. While rainfall variation alone doesn't capture true drought complexity, maximum temperature (Tmax) intensifies evapotranspiration, worsening water scarcity in mountainous areas like Astore and Dir, where SPEI-12 declined by -0.35 per decade. Longitudinal positioning strongly influences moisture: eastern stations

(Skardu, Gilgit) gain rainfall from orographic effects, but western sites (Chitral) stay dry due to distance from moisture sources. SPEI proved more effective than SPI for detecting temperature-sensitive droughts, showing 20-30% better accuracy at short timescales. MLR modeling confirmed Tmax and eastern longitude as key precipitation predictors, outperforming PLSR (RMSE:67.9 vs.69.7). Drought frequency surged dramatically, with Mangla recording 54 events (2001–2014) versus just 9 (1982–1990), signaling heightened climate vulnerability and drying across the basin. Mountainous regions should replace SPI with SPEI-based monitoring. Decision-makers must prioritize drought-resistant crops, robust water infrastructure, and early warning systems in hotspots. Future work should blend remote sensing with long-term datasets to improve predictive models. These findings offer a blueprint for sustainable water management in global mountain basins by translating mechanistic insights into actionable strategies.

Author Contributions

Haider Hassnain: conceptualization, methodology, analysis, writing – original draft, formal analysis. Muhammad Asad Hussain: conceptualization, review. Ali Hasan Jaffry: conceptualization, methodology, writing, review, and editing, Fakher Sherazi: review, editing, formal analysis. Anas Farooq: review. M Burhan: editing and review. Iqra Zainab: review.

Data Availability Statement

Data will be provided at request.

Conflict of Interest

The authors declare there is no conflict.

References

Adnan, M., Liu, S., Saifullah, M., Iqbal, M., Ali, A. F., and Mukhtar, M. A., 2022, August. Spatiotemporal variations in runoff and runoff components in response to climate change in a glacierized sub-basin of the Upper Indus Basin, Pakistan. Frontiers in Earth Science, 10. https://doi.org/10.3389/feart.2022.970349

Adnan, S., and Khan, A. H., 2009. Effective rainfall for irrigated agriculture plains of Pakistan. Pakistan Journal of Meteorology, 6(11), Pp. 61–72.

Ahmad, B., 2024, May. People's perception of climate change impacts on subtropical climatic region: A case study of Upper Indus, Pakistan. Climate, 12(5), Pp. 73. https://doi.org/10.3390/cli12050073

Ahmadzadeh, H., Mansouri, B., Fathian, F., and Vaheddoost, B., 2022, March. Assessment of water demand reliability using SWAT and RIBASIM models with respect to climate change and operational water projects. Agricultural Water Management, 261, 107377. https://doi.org/10.1016/j.agwat.2021.107377

Ansari, R., Liaqat, M. U., and Grossi, G., 2024, October. Improving flood and drought management in transboundary Upper Jhelum Basin-South Asia. Science of the Total Environment, 945, 174044. https://doi.org/10.1016/j.scitotenv.2024.174044

Ashraf, M. S., Shahid, M., Waseem, M., Azam, M., and Rahman, K. U., 2023, June. Assessment of variability in hydrological droughts using the improved innovative trend analysis method. Sustainability, 15(11), Pp. 9065. https://doi.org/10.3390/su15119065

Azam, M., and Khan, A. Q., 2016, May. Urbanization and environmental degradation: Evidence from four SAARC countries—Bangladesh, India, Pakistan, and Sri Lanka. Environmental Progress and Sustainable Energy, 35(3), Pp. 823–832. https://doi.org/10.1002/ep.12282

Baig, S., Sayama, T., and Yamada, M., 2022, September. Quantifying the changes in the runoff and its components across the Upper Indus River Basin under climate change. Journal of Water and Climate Change, 13(9), Pp. 3416–3434. https://doi.org/10.2166/wcc.2022.153

Climate and Development Knowledge Network and Germanwatch., 2020. Global Climate Risk Index 2020: Who suffers most from extreme weather events? Weather-related loss events in 2018 and 1999 to 2018.

Dubey, A., Swami, D., Gupta, V., and Joshi, N., 2023, August. From the peaks to the plains: Investigating the role of elevation in governing drought dynamics over the Indus River Basin. Atmospheric Research, 291, 106824. https://doi.org/10.1016/j.atmosres.2023.106824

Ficklin, D. L., Null, S. E., Abatzoglou, J. T., Novick, K. A., and Myers, D. T., 2022, March. Hydrological intensification will increase the complexity of water resource management. Earth's Future, 10(3). https://doi.org/10.1029/2021EF002487

Guttman, N. B., 1999. Accepting the Standardized Precipitation Index: A calculation algorithm. Journal of the American Water Resources Association, 35(2), Pp. 311–322.

Hamed, K. H., and Rao, A. R., 1998, January. A modified Mann-Kendall trend test for autocorrelated data. Journal of Hydrology, 204(1–4), Pp. 182–196. https://doi.org/10.1016/S0022-1694(97)00125-X

Hao, Z., Singh, V. P., and Xia, Y., 2018, March. Seasonal drought prediction: Advances, challenges, and future prospects. Reviews of Geophysics, 56(1), Pp. 108–141. https://doi.org/10.1002/2016RG000549

Hayes, M. J., Svoboda, M. D., Wilhite, D. A., and Vanyarkho, O. V., 1999, March. Monitoring the 1996 drought using the Standardized Precipitation Index. Bulletin of the American Meteorological Society, 80(3), Pp. 429–438. https://doi.org/10.1175/1520-0477(1999)080<0429:MTDUTS>2.0.CO;2

Hussain, A., Suliman, M., and Khan, F., 2024, August. Analysing spatiotemporal drought patterns in Punjab Province, Pakistan, utilizing SPI and SPEI. Theoretical and Applied Climatology, 155(8), Pp. 7867–7886. https://doi.org/10.1007/s00704-024-05090-7

Hussain, S., 2020, March. An overview on emerging water scarcity challenge in Pakistan, its consumption, causes, impacts and remedial measures. Big Data in Water Resources Engineering (BDWRE), 1(1), Pp. 22–31. https://doi.org/10.26480/bdwre.01.2020.22.31

IPCC., 2019. Climate Change and Land: An IPCC special report on climate change, desertification, land degradation, sustainable land management, food security, and greenhouse gas fluxes in terrestrial ecosystems. https://www.ipcc.ch/srccl/

Iqbal, M. M., 2022, January. Seasonal effect of agricultural pollutants on coastline environment: A case study of the southern estuarine water ecosystem of the Boseong County, Korea. Pakistan Journal of Agricultural Sciences, 59(1), Pp. 117–124. https://doi.org/10.21162/PAKJAS/22.7996

Iqbal, M. M., 2022, March. Analysis of seasonal variations in surface water quality over wet and dry regions. Water (Basel), 14(7), Pp. 1058. https://doi.org/10.3390/w14071058

Iqbal, M. M., 2023, January. Eutrophic status assessment based on very high-resolution satellite imagery in the coastline environment of Korea. Pollutants, 3(1), Pp. 59–73. https://doi.org/10.3390/pollutants3010006

Kamruzzaman, M., 2022, November. Spatiotemporal drought analysis in Bangladesh using the Standardized Precipitation Index (SPI) and Standardized Precipitation Evapotranspiration Index (SPEI). Scientific Reports, 12(1), 20694. https://doi.org/10.1038/s41598-022-24146-0

Lutz, A. F., Immerzeel, W. W., Kraaijenbrink, P. D. A., Shrestha, A. B., and Bierkens, M. F. P., 2016, November. Climate change impacts on the Upper Indus hydrology: Sources, shifts and extremes. PLoS One, 11(11), e0165630. https://doi.org/10.1371/journal.pone.0165630

Mahla, P., Lohani, A. K., Chandola, V. K., Thakur, A., Mishra, C. D., and Singh, A., 2019, April. Downscaling of precipitation using statistical downscaling model and multiple linear regression over Rajasthan State. Current World Environment, 14(1), Pp. 68–98. https://doi.org/10.12944/CWE.14.1.09

McKee, T. B., Doesken, N. J., and Kleist, J., 1993. The relationship of drought frequency and duration to time scales. Proceedings of the 8th Conference on Applied Climatology.

Mishra, A. K., and Singh, V. P., 2010, September). A review of drought concepts. Journal of Hydrology, 391(1–2), Pp. 202–216. https://doi.org/10.1016/j.jhydrol.2010.07.012

Novotny, E. V., and Stefan, H. G., 2007, February. Stream flow in Minnesota: Indicator of climate change. Journal of Hydrology, 334(3–4), Pp. 319–333. https://doi.org/10.1016/j.jhydrol.2006.10.011

Ougahi, J. H., Cutler, M. E. J., and Cook, S. J., 2022, February. Modelling

climate change impact on water resources of the Upper Indus Basin. Journal of Water and Climate Change, 13(2), Pp. 482–504. https://doi.org/10.2166/wcc.2021.233

Portela, M. M., dos Santos, J. F., Silva, A. T., Benitez, J. B., Frank, C., and Reichert, J. M., 2015. Drought analysis in southern Paraguay, Brazil and northern Argentina: Regionalization, occurrence rate and rainfall thresholds. Hydrology Research. https://doi.org/10.2166/nh.2014.074

Rafiq, M., 2024, August. Regional characterization of meteorological and agricultural drought in Baluchistan Province, Pakistan. PLoS One, 19(8), e0307147. https://doi.org/10.1371/journal.pone.0307147

Rafiq, M., Li, Y. C., Cheng, Y., Rahman, G., Zhao, Y., and Khan, H. U., 2023, November. Estimation of regional meteorological aridity and drought characteristics in Baluchistan province, Pakistan. PLoS One, 18(11), e0293073. https://doi.org/10.1371/journal.pone.0293073

Ramgopal, S., Dunnick, J., Owusu-Ansah, S., Siripong, N., Salcido, D. D., and Martin-Gill, C., 2019, November. Weather and temporal factors associated with use of emergency medical services. Prehospital Emergency Care, 23(6), Pp. 802–810. https://doi.org/10.1080/10903127.2019.1593563

Sebbar, B., 2024, December. Estimating evapotranspiration in mountainous water-limited regions from thermal infrared data: Comparison of two approaches based on energy balance and evaporative fraction. Remote Sensing of Environment, 315, 114481. https://doi.org/10.1016/j.rse.2024.114481

Sen, P. K., 1968. Estimates of the regression coefficient based on Kendall's tau. Journal of the American Statistical Association, 63(324), Pp. 1379–1389. https://doi.org/10.1080/01621459.1968.10480934

Tan, C., Yang, J., and Li, M., 2015, September. Temporal-spatial variation of drought indicated by SPI and SPEI in Ningxia Hui Autonomous Region, China. Atmosphere (Basel), 6(10), Pp. 1399–1421. https://doi.org/10.3390/atmos6101399

Thornthwaite, C. W., 1948, January. An approach toward a rational classification of climate. Geographical Review, 38(1), 55. https://doi.org/10.2307/210739

Van Fraassen, B. C., 1976. Probabilities of conditionals. In Foundations of Probability Theory, Statistical Inference, and Statistical Theories of Science: Volume I Foundations and Philosophy of Epistemic Applications of Probability Theory (pp. 261–308). https://doi.org/10.1007/978-94-010-1853-1_10

Vicente-Serrano, S. M., Beguería, S., and López-Moreno, J. I., 2010, April. A multiscalar drought index sensitive to global warming: The Standardized Precipitation Evapotranspiration Index. Journal of Climate, 23(7), Pp. 1696–1718. https://doi.org/10.1175/2009JCLI2909.1

Waheed, A., Jamal, M. H., Javed, M. F., and Muhammad, K. I., 2024, April. A CMIP6 multi-model based analysis of potential climate change effects on watershed runoff using SWAT model: A case study of Kunhar River Basin, Pakistan. Heliyon, 10(8), e28951. https://doi.org/10.1016/j.heliyon.2024.e28951

Yevjevich, V., 1967. An objective approach to definitions and investigations to continental hydrologic droughts. Colorado State University.

Zafar, U., 2024, October. Analyzing the spatiotemporal changes in climatic extremes in cold and mountainous environment: Insights from the Himalayan mountains of Pakistan. Atmosphere (Basel), 15(10), 1221. https://doi.org/10.3390/atmos15101221

Zhou, W., Xian, F., Du, Y., Kong, X., and Wu, Z., 2014. The last 130 ka precipitation reconstruction from Chinese loess ^10Be . Journal of Geophysical Research: Solid Earth, 119(1), Pp. 191–197. https://doi.org/10.1002/2013JB010296